

A HYBRID POWER GENERATION AND REFRIGERATION CYCLE WITH AMMONIA-WATER MIXTURE

Yoshiharu AMANO, Visiting Research Lecturer
Advanced Research Institute for Science and
Engineering, Waseda University

Takumi HASHIZUME, Professor
Advanced Research Institute for Science and
Engineering, Waseda University

Yoshihaki Tanzawa, Lecturer
Department of Mechanical Engineering,
Nippon Institute of Technology

Takashi SUZUKI, Student
Graduate school of Science and Engineering,
Waseda University

Masashi AKIBA, Visiting Professor
Advanced Research Institute for Science and
Engineering, Waseda University

Akira USUI, General Manager
Environmental Engineering Group,
Ebara Corporation

ABSTRACT

To prevent the destruction of environment, natural working fluids such as water, ammonia and other organic refrigerants have been getting a lot of attention these days. With increased regulation being placed upon the use of chlorofluorocarbon-based (CFC) refrigerants, and the phase out of CFCs and hydrofluorocarbons (HCFCs) altogether, alternative refrigerants for use in existing refrigeration packages and systems are actively being investigated. Ammonia is one alternative refrigerant for new and existing large centralized refrigerating and air-conditioning system. On power generation, Kalina cycle, which employs Ammonia-water mixture(AWM) as working fluid, also make researchers attention to ammonia.

An hybrid power generating and refrigerating cycle with ammonia-water mixture is proposed in the paper. An AWM turbine cycle and a single-effect ammonia-absorption refrigeration cycle are connected to expand the availability of ammonia-absorption refrigerating cycle. To reduce the heat of rectification ammonia-rich liquid is fed from the AWM turbine cycle¹⁾. Simulation model for the hybrid system is developed to investigate the cycle efficiency. The results of the simulation shows that the hybrid system performs 9% to 13.3% higher COP of the refrigeration cycle and also 9% to 13.3% higher net system output of the turbine system compared with the separate operation of power generating and refrigerating cycle.

The AWM turbine system and the absorption refrigerator are constructed to demonstrate the availability for experimental test.

INTRODUCTION

The authors have been studied on dynamic characteristics of a Low boiling-temperature medium Turbine System (LTS) which employs R11, R123, R134a or mixture of R123 and R134a (Tanzawa et al., 1998) as a working fluid.

Kalina cycle is one of several novel plant designs that have exhibited the potential for high thermal efficiency relative to the Rankine cycle (Omen and Shaw, 1986; Stambler, 1995). Kalina cycle technology is used to increase the efficiency of power plants by increasing the average temperature of heat acquisition by working fluid and the reducing the amount of heat rejected to the environment in the stack gas or cooling water (Kalina and Tribus, 1992). These goals are achieved by using a working fluid composed of an ammonia-water mixture, rather than only water. When the ammonia-water mixture liquid is heated, volatile ammonia tends to vaporize first at a lower temperature rather than water. The temperature of the remaining saturated liquid rises as the ammonia concentration decreases. The property of AWM makes a better match to the enthalpy-temperature curve of sensible heat source such as hot gas heat source or hot water. Thus the Kalina cycle shows higher gross output power rather than that of conventional steam turbine systems.

The paper illustrates that the reason why the hybrid configuration is effective to the low temperature heat source around 100 to 200 [°C] with simulation results.

NOMENCLATURE

SYMBOL:

G	mass flow rate	[kg/s]
h	specific enthalpy	[kJ/kg K]
P	pressure	[MPa] abs.
Q	heating rate	[kW]
T	temperature	[°C]
W	output power	[kW]
z	ammonia mass fraction	[kg/kg]

Subscript:

E:	Evaporator
D:	Desorber
R:	Reflux or Rectification
S:	Heat source
SYS:	System

SYSTEM CHARACTERISTICS

The hybrid power generating and refrigerating system is composed of two cycles, that is, an AWM turbine cycle and an ammonia absorption refrigeration cycle. These two cycles are heated by common low-temperature waste heat source such as low pressure process steam, exhaust gas, hot water and so on(see fig. 1). These two cycles can be driven independently. However, the hybrid system is able to produce more power with sharing the working fluid, AWM.

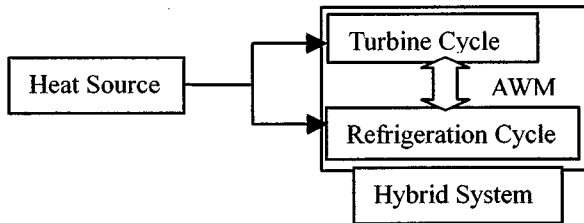


Fig. 1 Hybrid system

Ammonia Absorption Refrigerator: AAR

The ammonia absorption refrigeration cycle is single-stage absorption type as shown in fig.2. The evaporator saturation temperature at the outlet is assumed to be T_E [°C] with saturated vapor leaving. The mass flow rate of solution through solution pump is G_s [kg/s]. The mass flow rate of the bleed saturated vapor and saturated liquid from bleed heat exchanger are G_b'' [kg/s] and G_b' [kg/s]. The rectifying column produces a vapor with a mass fraction of 0.998. The mass flow rate of lean solution at the outlet(point 1) of the desorber is G_a [kg/s]. The mass flow rate feed to rectifying column is G_r [kg/s] and reflux low rate from condenser to rectifying column is G_R [kg/s]. G_K [kg/s] is the mass flow rate of rectified liquid.

The COP(Coefficient of Performance) is defined by the equation (1).

$$COP = \frac{Q_E}{Q_D} \quad (1)$$

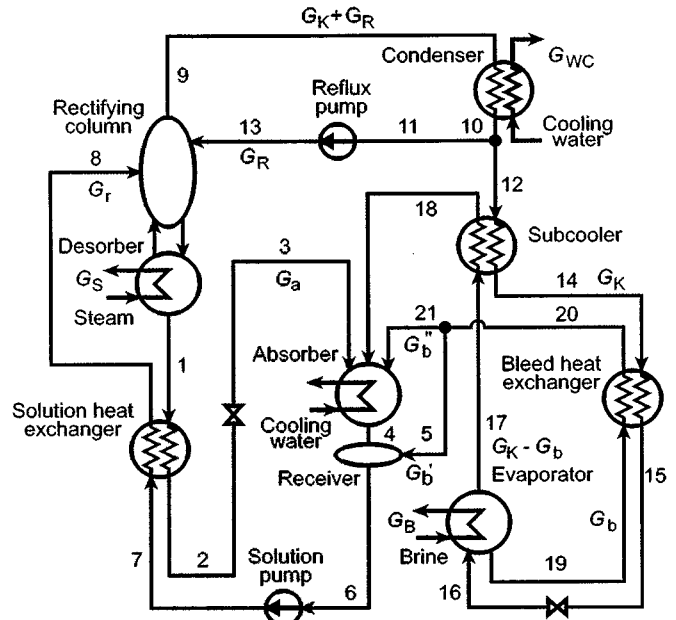


Fig.2 Flow sheet of single-effect ammonia absorption refrigeration cycle.

Table 1 The specifications of AAR.

Item	Specifications
Evaporating temperature	-10 °C
Cooling capacity	100 USRT
Heat source	Steam sat.(0.59 MPa.gage)
Cooling water temperature	Inlet: 32 °C
Ammonia mass fraction of rectified vapor	0.998 kg/kg
Efficiency of rectification	0.8

The energy balance equations at the desorber and rectifying column are as follows:

$$\begin{aligned}
 Q_D &= (G_K + G_R)h_9 + G_a h_1 - G_R h_{13} - G_r h_8 \\
 &= G_R (h_9 - h_{13}) + G_K h_9 + G_a h_1 - G_r h_8 \\
 &= Q_R + G_K (h_9 - h_1) + G_r (h_1 - h_8) \quad (2)
 \end{aligned}$$

Where, Q_R is the heat of rectification.

The equations (1) and (2) show that the reduction of heat of rectification means high COP because of the reduction of Q_D . It follows that the mass flow rate of the heat source tends to be small. As a result, the more heat source could be provided to the turbine cycle.

There are several means to decrease Q_D :

- (1) Decrease h_9 .
- (2) Decrease Q_R .
- (3) Decrease G_r .

(4) Decrease the specific enthalpy difference (h_1-h_8). This means the decrease of heat-exchange loss at solution heat exchanger.

Figure 3 shows that the specific enthalpy of vapor at the state point of 9 versus saturated vapor pressure. The specifications of the AAR is listed on the table 1. The fig. 3 shows that there is a maximum point at $P=1.23$ [MPa], so you should avoid the pressure point. However the corresponding pressure is determined by the condensing pressure, and the condensing pressure is derived from evaporating pressure at evaporator. Therefore, the specific pressure h_9 is fixed by the evaporating pressure. The mechanism is illustrated by the Dühling plot in fig. 4.

The heat of rectification is deeply depend on the ammonia mass fraction of the solution: z_8 . Figure 5 shows the theoretical heat of rectification Q_{Rth} versus ammonia mass fraction z_8 . From the energy and mass balance equations at the desorber and rectifying column, the following equation (3) is derived.

$$G_r = \frac{z_9 - z_1}{z_8 - z_1} G_K \quad (3)$$

The equation also shows that the high-ammonia mass fraction at the state 8 contributes the decrease of the G_r . The enthalpy difference between the state of point 1 and 8 (h_1-h_8) tends to be small when the difference of the ammonia mass fractions i.e., $z_8 - z_1$ decrease. Figure 5 is the enthalpy-mass fraction diagram. This diagram shows that the increasing of the mass fraction of the state point 8 decrease the theoretical heat of rectification.

The challenge is now to make the ammonia rich solution at the state point of 8 to feed rectifying column. One of the answer is to supply ammonia rich solution to the point from other cycle, i.e., the AWM turbine cycle.

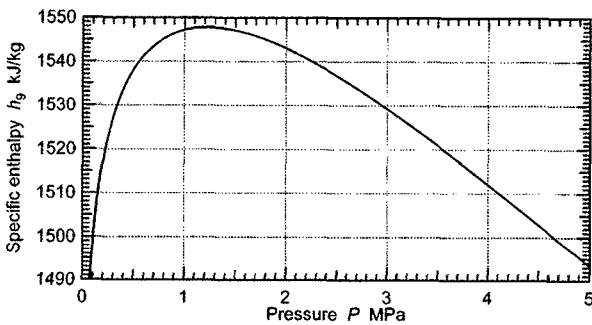


Fig.3 Specific enthalpy versus saturation vapor pressure

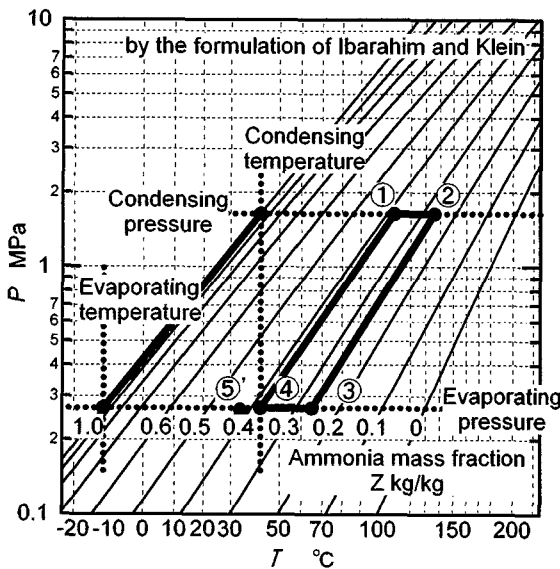


Fig.4 Dühling plot of cycle solution in AAR.

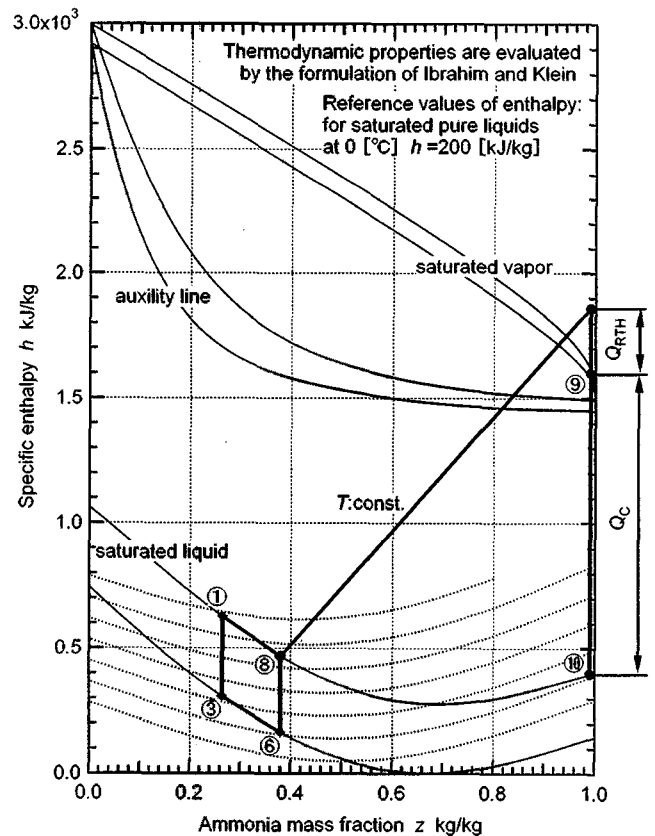


Fig. 5 Enthalpy-mass fraction diagram.

Ammonia-Water Mixture Turbine System: AWMTS

The configurations of AWMTS (Amano et. al., 1999) are illustrated in Fig.6. The system features two simple Kalina cycle systems, KCS-1 and KCS-34. KCS-1 is one of the simplest Kalina cycle which has a distillation/condensation subsystem (DCSS). KCS-34 is another simple Kalina cycle that is mainly utilized for geothermal source plant which has a vapor generator subsystem. In the vapor generator subsystem, liquid preheating, vaporization and separation of saturated vapor and liquid at the separator are achieved. KCS-1 is effective to heat source at a temperature between 200 and 400 [°C]. KCS-34 is effective at heat source at a temperature between 100 and 200 [°C]. The AWMTS has both of the two subsystems, e.g., the vapor generator subsystem and the distillation-condensation subsystem. The turbine system configuration is designed for low-pressure process steam as heat source.

There are 7 levels of ammonia mass fraction in the turbine cycle (see Table 2). This is applicable to share the AWM with AAR cycle.

Table 2 Ammonia mass fraction of the state points.

State points in Fig. 6	Nominal mass fraction kg/kg
10	0.94
1, 2, 3	0.71
14, 15, 16, 17, 18, 23	0.6
4, 5, 6, 7, 8, 9	0.43
11, 12, 13	0.30
22	0.28
19, 20, 21	0.17

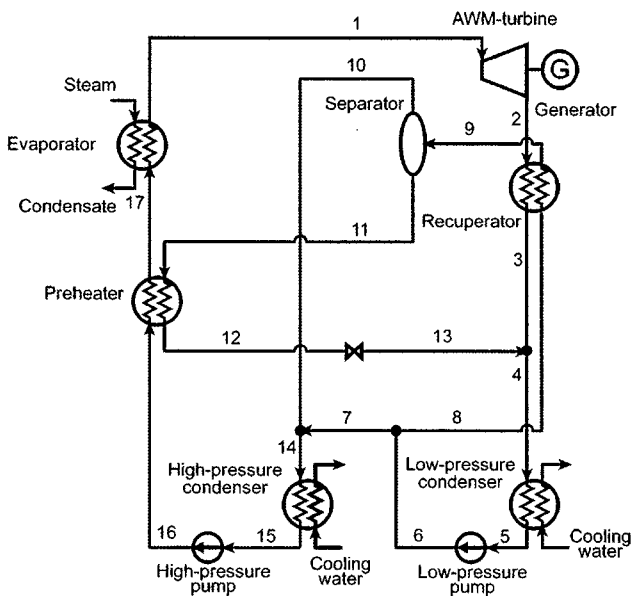


Fig. 6 Flow sheet of the AWMTS.

Figures 7, 8 and 9 show the system output power characteristics. The output power is calculated as maximum power to the parameters. For example, in fig.7, These figures represent that the characteristics of the AWMTS is deeply depend on the following variables:

- (1) Temperature at the inlet of the separator-2 : T_9
The fig. 7 shows that there is a maximum output power at a T_9 .
- (2) Turbine inlet pressure P_1
The fig. 8 also shows that the maximum point at a P_1 .
- (3) The ammonia mass fraction at evaporator outlet, i.e., of the state point of 18.

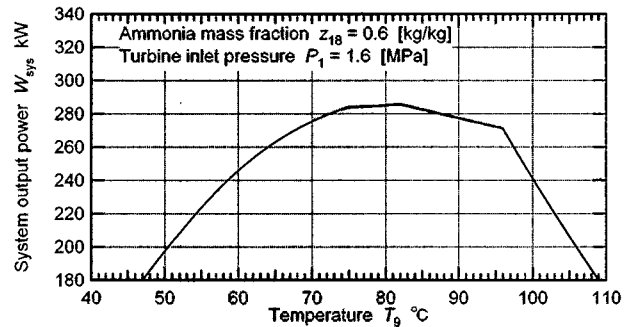


Fig. 7 System output power versus temperature at the inlet of the separator-2.

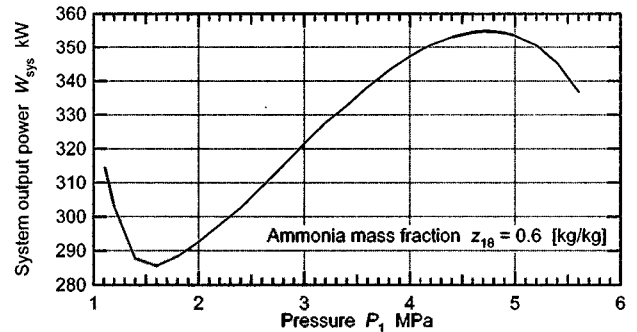


Fig. 8 System output power versus turbine inlet pressure.

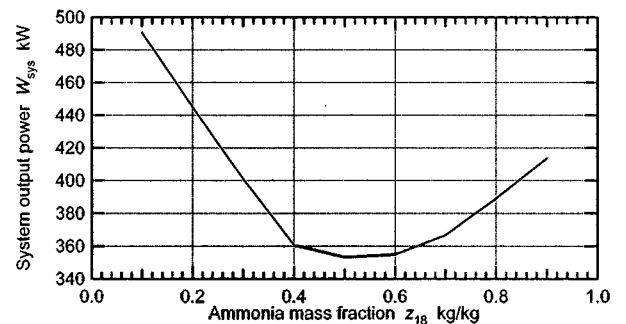


Fig. 9 System output power versus evaporator outlet ammonia mass fraction.

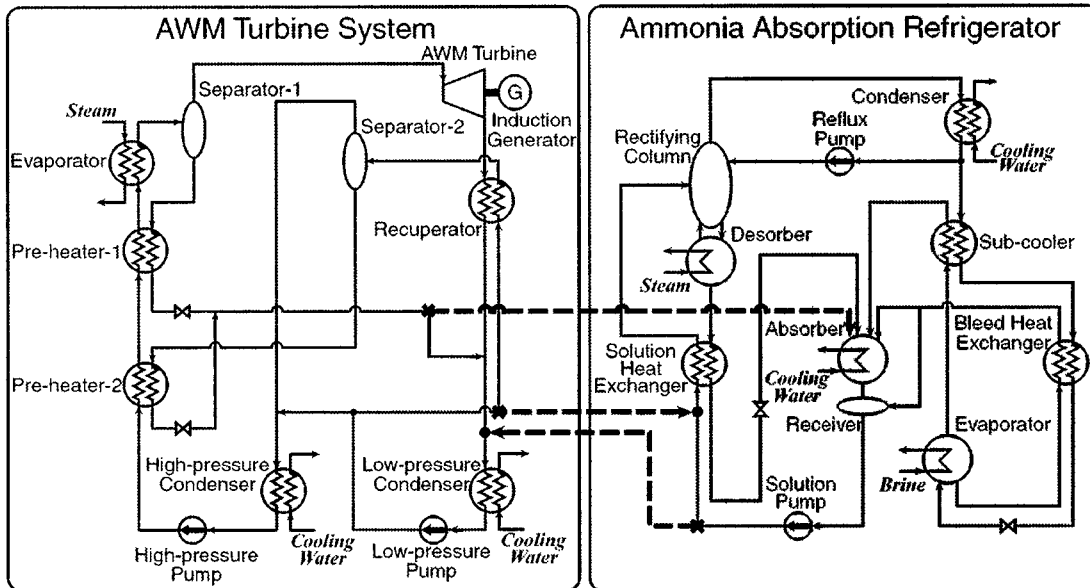


Fig. 10 Flow sheet of the hybrid configuration of the AWM Turbine System and Ammonia Absorption Refrigerator.

Hybrid Configuration

Figure 10 shows the hybrid configuration of the two cycles: AWM Turbine System and AAR. To maintain the mass balance, dashed three lines are connected to each other to sharing the working fluid. In this configuration, simulation model was constructed. The thermodynamic properties of the AWM are calculated with the PROPATH ver 11.1 which is based on the literature (Ibrahim and Klein, 1993).

The assumptions for the calculation are following:

[common]

Cooling water: inlet: 32 [°C] / outlet: 37 [°C]
 Heat source: dry sat. steam/
 0.69 [MPa.abs] / 2200 [kg/h]

[AAR]

Desorber outlet: 130 [°C]
 Absorber outlet: 42 [°C]
 Evaporating temperature: -10 [°C]
 Mass fraction of bleed: 0.960 [kg/kg]
 Efficiency of rectification: 0.8
 Cooling capacity: 100 USRT

[AWMTS]

Turbine/pump efficiency: 1.0
 Pinch point temperature difference at heat exchangers: 10 [°C]

The characteristics of the hybrid configuration and separate configuration. The separate configuration of the two cycles does not share AWM and share the same heat source to keep cooling capacity is 100 USRT. First, applicable range of the ammonia mass fraction at the outlet of the evaporator in AWM Turbine System (z_{IN}) is investigated. The result is from 0.4 to 0.6 [kg/kg]. Next, the system output power versus AWM temperature at the inlet of the separator-2 in AWM Turbine System (T_{SP-2}) is investigated. The results

are shown in the fig. 11. The figure shows that the system output power is maximum at $z_{IN} = 0.45$ [kg/kg] and $T_{SP-2} = 53 \sim 62$ [°C]. It is about 13.3% higher than that of the separate configuration. Figure 12 shows the relationship between the output power and turbine inlet pressure P_{IN} in the case of $z_{IN} = 0.45$ [kg/kg]. When the P_{IN} is about 2.8 [MPa.abs], the system output power is

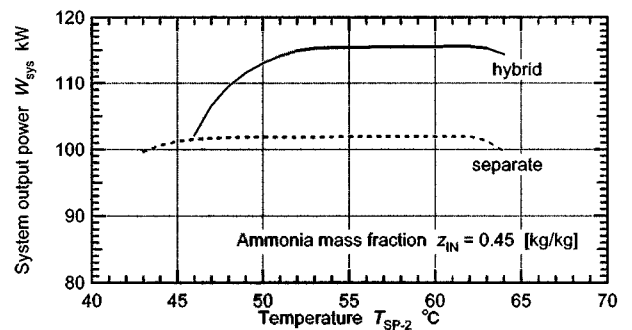


Fig. 11 System output versus temperature at the inlet of the separator-2 ($z_{IN} = 0.45$ [kg/kg])

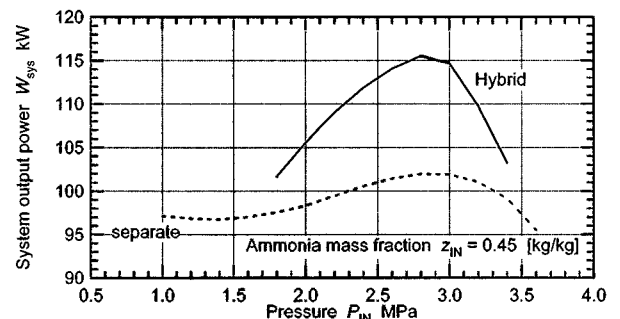


Fig. 12 System output versus turbine inlet pressure ($z_{IN} = 0.45$ [kg/kg])

maximum value. In the case, the heat of rectification is decreased that is shown in fig.13. The COP of the AAR is represented in fig.14. In those case, other parameters such as turbine inlet pressure and so on are selected to produce maximum output power to the parameter of the bottom axis of the figures 11 to 14.

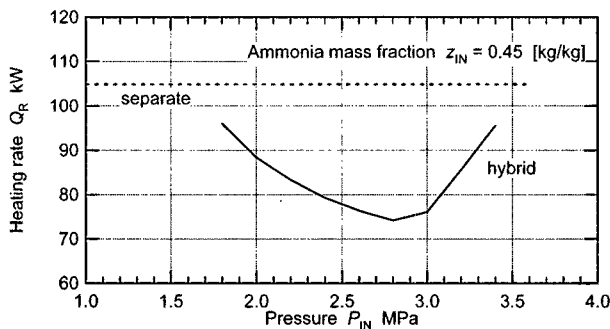


Fig. 13 Heat of rectification versus turbine inlet pressure ($z_{IN} = 0.45$ [kg/kg]).

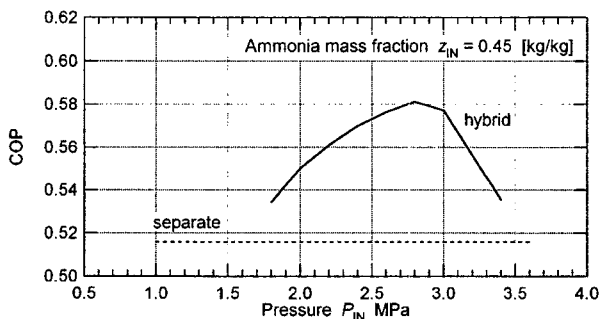


Fig. 14 COP of the AAR versus turbine inlet pressure ($z_{IN} = 0.45$ [kg/kg]).

CONCLUSION

The simulation results show that the hybrid configuration produces 13.3 % higher output power and COP than those of the separate configuration because of the decrease of heat of rectification in AAR with sharing the working fluid. In the hybrid configuration, only the operating condition of the solution cycles in AAR and AWMTS are altered from the separate configuration.

REFERENCES

- 1) Amano, Y., Tanzawa, Y., and et. al., "MODELING AND EXPERIMENTAL INVESTIGATION OF DYNAMICS OF A DIRECTLY COMBINED BINARY TURBINE SYSTEM USING A MIXTURE (R134a/R123)" Proc. Renewable and Advanced Energy Systems for the 21st Century / ASME RAES99-7647 No.25 (1999) pp.1-6.
- 2) Amano, Y., et. al., "Effectiveness of an ammonia-water mixture turbine system to hot water heat source" Proc. 1999 IJPGC-ICOPE ASME/JSME PWR-Vol.34 vol.2 (1999), pp.67-73.
- 3) Enick, Robert M., et. al., "The Modeling of LEBS-Kalina Power Cycles," Proc. 1997 IJPGC PWR-Vol.32(2), ASME (1997), pp.55-67.
- 4) Ibrahim, O.M., and Klein, S.A., "Thermodynamic Properties of Ammonia-Water Mixtures," ASHRAE Trans. 99, (1993), pp.1495-1502.
- 5) Kalina, A. and Tribus, M., "Advances in Kalina Cycle Technology (1980-1991): Part II Iterative Improvements," Proc. Of the Florence World Energy Res. Symp., Firenze, Italy, (1992), pp.111-125.
- 6) Mathias, P.M., "A Versatile Phase Equilibrium Equation of State," Ind. Chem. Process Des. Dev., Vol.22, (1983), pp.385-391.
- 7) Oman, H and Shaw, R., "Routes to 50 Percent Efficiency in Heat Engines," ACS publication 869097 (1986), pp.326-330.
- 8) Tanzawa, Y., et al., "Modeling and Experimental Investigation of Dynamics of A Directly Combined Binary Turbine System Using Steam and R123," Proc. IMECE'98 AES-vol.38, (1998), p35-40.
- 9) Tillner-Roth, Reiner and Friend, Daniel G., "A Helmholtz Free Energy Formulation of the Thermodynamic Properties of the Mixture {Water + Ammonia}," J. Phys. Chem. Ref. Data 27, 63 (1998), pp63-97.
- 10) Stambler, I., "Kalina Cycle Provides 25% More Power and 3 % Better Net Efficiency," Gas Turbine World (July-August 1995), pp.38-41.
- 11) Schwartzentruber, J. and Renon, H., "Extension of UNIFAC to Higher Pressures and Temperatures by Use of a Cubic Equation of State," Ind. Eng. Chem. Res., Vol.28 (1989), pp.1049-1055.
- 12) Ziegler, B, and Trepp, C., "Equation of State for Ammonia-Water Mixtures," int.J.Refriger. 7(2), (1984), pp.101-106.